

BRL R 1456

B R L

File copy
AD 1456-31-1

REPORT NO. 1456

VAPORIZATION WAVE TRANSITIONS

by

F. D. Bennett

November 1969

This document has been approved for public release and sale;
its distribution is unlimited.

U.S. ARMY ABERDEEN RESEARCH AND DEVELOPMENT CENTER
BALLISTIC RESEARCH LABORATORIES
ABERDEEN PROVING GROUND, MARYLAND

Destroy this report when it is no longer needed.
Do not return it to the originator.

The findings in this report are not to be construed as
an official Department of the Army position, unless
so designated by other authorized documents.

B A L L I S T I C R E S E A R C H L A B O R A T O R I E S

REPORT NO. 1456

NOVEMBER 1969

VAPORIZATION WAVE TRANSITIONS

F. D. Bennett

Exterior Ballistics Laboratory

This document has been approved for public release and sale;
its distribution is unlimited.

RDT&E Project No. 1T061102A33D

A B E R D E E N P R O V I N C E G R O U N D, M A R Y L A N D

B A L L I S T I C R E S E A R C H L A B O R A T O R I E S

REPORT NO. 1456

FDBennett/jah
Aberdeen Proving Ground, Md.
November 1969

VAPORIZATION WAVE TRANSITIONS*

ABSTRACT

A vaporization wave analogous to the unsteady simple wave in an expanding gas is proposed to account for phenomena observed in the evaporation of superheated metals. The vaporizing model is visualized on thermodynamic grounds as carrying the liquid metal through a continuous succession of states either on or near the liquidus line in the two-phase region. On this line, the adiabatic sound speed for wet vapor will limit the rate of propagation of the vaporization front

**This report contains the essence of two lectures given by the author to the International School of Physics "Enrico Fermi" Course on Physics of High Energy Density, 1969, Varenna, Italy.*

into the liquid. Experimental data for wire explosions of Al, Ag, Cu, Au, Pb and Hg (frozen) are analyzed for wave speeds. While the influence of thermal expansion of the liquid can be accounted for theoretically, insufficient thermal data are available for the metals to permit correction of the wave speeds for this effect. The experimentally derived wave speeds are compared with theoretical values of the adiabatic sound speed in the wet vapor obtained from a modified van der Waals equation of state. At low velocities, the agreement is satisfactory but higher values deviate considerably from theory. Possible causes of the deviations include the crudity of the fluid dynamic model, neglect of thermal expansion, lack of information about the relationship between density and electrical conductivity and the approximation imposed by the van der Waals equation.

TABLE OF CONTENTS

	Page
ABSTRACT	3
LIST OF ILLUSTRATIONS.	7
1. INTRODUCTION	9
2. WAVE HYPOTHESIS.	10
3. EXPLODING WIRE EXPERIMENTS	12
4. CONSTANT VELOCITY VAPORIZATION WAVES	13
5. WAVE SPEEDS FROM EXPERIMENTS	14
6. THERMODYNAMIC MODEL.	17
7. COMPARISON OF THE THERMODYNAMIC MODEL WITH EXPERIMENT.	22
8. DEVIATIONS FROM THE MODEL.	24
REFERENCES	29
DISTRIBUTION LIST.	31

LIST OF ILLUSTRATIONS

Figure		Page
1	Sketch of two-phase region and isotherms. P - pressure, V - specific volume.	26
2	Streak photograph of expanding copper wire correlated in time with current and voltage. $d = .0254 \text{ cm}$, $V_0 = 3 \text{ kV}$, $C = 32 \mu\text{F}$.	27
3	Wave speeds for several metals.	28

1. INTRODUCTION

We outline here some theoretical and experimental aspects of the dynamical process by which an impulsively heated fluid makes the transition from liquid to vapor. Our interest is in the initial stages of the expansion as it occurs in the vaporization of superheated metals.

For polytropic, non-reacting fluid the head of an expansion wave proceeds into the compressed region at the local velocity of sound and the ensuing expansion is a simple wave.¹ When the fluid can be condensed, the first expansion will also be limited by the speed of sound in the liquid; but the vaporization which follows may take place either from the bounding, external surface or by cavitation with vapor bubble formation. Since formation of internal cavities is limited by inertia and nonequilibrium effects, and may require a considerable time interval for bubble formation, we shall consider only experimental situations where vaporization takes place from the exposed surface. In this case the evaporation will be limited by some maximum speed with which the head of the wave travels. Because a phase change occurs and because the resulting damp vapor is more compressible than the liquid, one would expect the limiting wave speed to be much slower than that of sound in the homogeneous liquid. In other words, the rate at which a uniform vaporization phenomenon should occur will be much slower than the rate at which a purely liquid expansion is propagated.

**References are listed on page 29.*

2. WAVE HYPOTHESIS

We wish to test the hypothesis that the limiting upper velocity of a dynamic vaporization process will be a sound speed characteristic of the two-phase region of the fluid. In particular the chosen speed will be that of the coexistence side of the liquidus line which is the low volume boundary of the two-phase region, represented as the locus $V_s(T)$ in Figure 1.

For a substance characterized by an equation of state $P = P(V, T)$, where $V = 1/\rho$ is specific volume and P , ρ , T refer to pressure, density and temperature respectively, one can readily show^{2,3} that the speed, c , of a small disturbance is given by $c^2 = (\partial P / \partial \rho)_s$, or equivalently by

$$c^2 = (\partial P / \partial \rho)_T + (T / \rho^2 C_V) (\partial P / \partial T)_{\rho}^2 , \quad (1)$$

where C_V is the specific heat at constant volume. We note that within the two-phase region the number of free variables is reduced to one and $P = P(T)$, the vapor pressure; thus, only the second term of Equation (1) remains and,

$$c = (T / C_V \rho^2)^{1/2} (dP / dT) . \quad (2)$$

On the boundary given by the liquidus line two values of sound speed occur, viz., those for the liquid and liquid plus damp vapor. Sound speed is double valued on the loci where slope discontinuities occur in the adiabats.

We refine the wave hypothesis slightly, to state: dynamic vaporization phenomena in superheated liquids move into the undisturbed fluid no more rapidly than the liquid-vapor sound speed characteristic of the liquidus line. A more detailed development of the thermodynamical model will be given in § 6 below.

While our main experience with the vaporization waves comes from experiments with metals, one would expect the hypothesis to apply equally well to a broader class of liquids including elements, compounds, solutions and mixtures. Necessary conditions for any liquid to exhibit vaporization wave phenomena can be tentatively stated as follows. Such a substance should have 1) a piecewise continuous equation of state relating pressure, specific volume and temperature, 2) a change in phase with a large increase in specific volume, 3) a latent heat of vaporization large compared with the specific energy at the boiling point; and, for practical reasons, 4) a temperature high enough so that specific energy exceeds a certain threshold.

Wave-like vaporization phenomena are encountered in the steam shock tube. Here, water contained at temperatures and pressures higher than its normal boiling point is suddenly released, by breaking a diaphragm, into a driven section containing air or other gas at lower pressure. Experiments of this kind have been performed by Brown⁴ and by Terner.⁵ Brown treats the expansion wave traveling into the driver by assuming a two-stage process. In the first stage the water over-expands to a lower-pressure, metastable state. In the second it undergoes an exponential relaxation with increase of specific volume to its final equilibrium state. The connection between metastable and equilibrium states is found by using certain additional assumptions and the conservation laws of fluid mechanics in their "jump" form. While there is some arbitrariness about choosing the metastable state, Brown's experimental data appear to agree somewhat better with the results of the two-stage theory than with those of an equivalent equilibrium expansion.

3. EXPLODING WIRE EXPERIMENTS

From the point of view of historical order, the vaporization wave hypothesis was first developed³ to account for some of the peculiar phenomena observed when wires are exploded by a condenser discharge. Somewhat later⁶ it was proposed as a more general concept applying to the explosive expansion of superheated liquids in general.

In an exploding wire experiment a long, thin, conducting cylinder is impulsively heated by an energetic condenser discharge. Depending on the choice of the conductor and the initial conditions a variety of complex phenomena occur in the ensuing expansion. We shall not describe the entire process here but for a more complete discussion refer the reader to a recent review.⁷ What will interest us are the early stages of the explosion as depicted in Figure 2. There one sees a streak camera record of the expansion of a cylinder of copper correlated in time with simultaneous oscilloscope traces of the current passing through the wire and the voltage measured across it. The small ramp in the voltage curve represents melting of the wire. Shortly thereafter the streak photograph shows a haze of vapor expanding about the more-dense, interior of the wire. During this process the current decays rapidly to zero in the same interval that voltage goes through a peak, which in this case is about four times as high as the initial condenser voltage. For the example chosen, the wire is so well matched to the condenser that nearly the entire initial energy is deposited during the first pulse. The physical evidence for a vaporization wave is contained in the interval of wedge-shaped expansion terminated by the zero of the current pulse.

An interpretation of the exploding wire data can be obtained as follows. To first approximation we suppose the wire material to exist in two states only, viz., (1) fully conducting metal not yet affected by the expansion wave, and (2) expanded, nonconducting, wet vapor. Thus, for a vaporization wave propagating with velocity $v(t)$

inward from the wire periphery, the radius of the conducting core diminishes with time as $r = r_0 [1 - \int_{t_0}^t (v(\xi)/r_0) d\xi]$, where t_0 is the time chosen to represent the start of the expansion. In the example of Figure 2, t_0 would be a little more than 4 μ sec. With this model, conduction will cease when $r = 0$. Thus, the model provides an interpretation of the current shut-off; and, in fact, initiates an explanation of dwell.

4. CONSTANT VELOCITY VAPORIZATION WAVES

Since wire resistance, R , varies inversely with area of cross section we can write

$$R = R_0(T) [1 - \int_{t_0}^t (v(\xi)/r_0) d\xi]^{-2} . \quad (3)$$

If, for simplicity, we neglect temperature effects and assume the wave speed to be constant; then, with $\tau = r_0/v$ and $s\tau = t - t_0$, Equation (3) becomes

$$R = R_0 / (1-s)^2 . \quad (4)$$

As Figure 2 shows, the expansion takes place in a short time interval near the maximum of current. When current is at its maximum the charge on the condenser is zero and the energy supply is stored in the magnetic field. If we assume condenser voltage to be negligible during the current decay, the circuit equation becomes $L(di/dt) + Ri = 0$; and, with the previous work, can be written

$$di/ds + ai/(1-s)^2 = 0 , \quad (5)$$

where $a = (r_0/v)(R_0/L)$ is the ratio of the time constant of the wave to that of the circuit. Integrating Equation (5) yields

$$i = i_0 \exp[-as/(1-s)] , \quad (6)$$

and with the definitions for voltage, V_R and power, P_R ,

$$V_R = R_0 i_0 (1-s)^{-2} \exp[-as/(1-s)] \quad , \quad (7)$$

and

$$P_R = R_0 i_0^2 (1-s)^{-2} \exp[-2as/(1-s)]. \quad . \quad (8)$$

Differentiation shows that V_R and P_R have maxima at $1 - a/2$ and $1 - a$ respectively. Furthermore, these maxima have their minimum values, as functions of a , at $a = 2$ and $a = 1$ respectively. A variety of different pulse shapes can be interpreted with this elementary calculation. Broadly speaking, if the time for e-fold decay of current is small compared with the time of wave passage, i.e., $a > 2$, the current and voltage decay curves have exponential shapes without peaks. Conversely, if $a < 1$ and the wave is comparatively fast, then the current decay is quite flat at first and steepens rapidly as the wave approaches the center. Voltage passes through a peak whose height increases as a gets smaller. The present treatment can be generalized to any portion of the current cycle providing only that the vaporization wave relaxation time is much smaller than a quarter period of the undamped circuit so that the condenser voltage can reasonably be taken constant. The analysis of the constant speed vaporization wave shows clearly the interrelation between circuit and wave speed parameters; and shows, furthermore, the possibility of a unified discussion of a wide variety of pulse shapes. It fails to provide an accurate method of calculating actual wave speeds.

5. WAVE SPEEDS FROM EXPERIMENTS

If one abandons the program, initiated with the discussion of constant speed waves, of attempting to provide a wave-speed theory of current and voltage pulses, a considerable shift in point of view becomes possible. We regard the $i-V_R$ curves as the raw data, the physical evidence of the vaporization wave, and attempt to deduce wave

speeds from them. Several additional assumptions must be made in order to provide a rational reduction scheme. We outline it here; the details may be found elsewhere.^{3,9}

If we neglect all work and heat terms except Ohmic heating, conservation of energy allows us to equate rise in specific energy of the current-carrying core with the electrical energy deposited. From the corrected voltage V_R and current i curves one can calculate

resistance $R = V_R/i$, power $P_R = V_R i$ and energy $E = \int V_R i dt$. We can .

write

$$de = i^2 R dt/m , \quad (9)$$

$$= V_R^2 dt/Rm , \quad (10)$$

where e , m are respectively the specific energy, and the mass heated during interval dt . The quantity Rm is an invariant under the vaporization wave. The factor $(r/r_0)^2$ cancels out of the product; however, temperature variation remains and must be accounted for.

To this end we further assume that resistance is linear with specific energy above the melting point. This assumption can be expressed by writing

$$R = R_0 [1 + \beta (e - e_0)] (r_0/r)^2 , \quad (11)$$

where β is a constant to be determined from the experiment. If specific heat s is constant in the interval, then $\beta = \alpha/s$, $e = sT$ and Equation (11) contains the usual statement that resistance increases linearly with temperature. Using Equations (10) and (11) and integrating, we find

$$(e - e_0) + (\beta/2)(e - e_0)^2 = (1/m_0 R_0) \int_{t_0}^t V_R^2 dt . \quad (12)$$

To determine time t_0 when the vaporization wave begins, one plots scaled resistance, or resistivity, against apparent specific energy E/m_0 . Before vaporization, the radius is taken to be $r = r_0$ and the constant β in Equation (11) can be determined from the linear portion of the resistivity data above melt. After vaporization commences, R rises steeply away from the linear law and this law is extrapolated to account for the effects of temperature variation. The point at which R departs from the line determines R_0 and e_0 . Since R is already known as a function of time t_0 is then determined. True (e,t) values may be obtained by integrating V_R^2 as in Equation (12); and (e,R) values by comparison with the (R,t) data. With (e,R) data Equation (11) may be solved for $(r/r_0)^2$. The resulting points are fitted to an interpolation curve and differentiated numerically to obtain wave speed. The initial radius r_0 is taken nominally to be that of the cold wire. A more elaborate reduction method has been devised⁹ to correct for thermal expansion of the liquid cylinder; but, because thermodynamic data for metals at high temperatures are lacking, has not yet been used. The correction if it could be made would tend to increase the values of wave speed deduced from measurement by a variable factor which increases approximately from 1 at room temperature to 1.7 at the critical temperature.

The assumption of a linear dependence of resistivity on specific energy is crucial to the reduction. Without it no account can be taken of the effects of temperature rise, and these are known to be too large to neglect. Certain metals, e.g., Fe, Ni, W show anomalous decreases of resistance above the melting point in an exploding wire experiment. For this reason no wave speeds have yet been obtained for these metals or for others like them. If, as suspected, the cause lies in early voltage breakdown and associated current conduction in paths external to the wire there is some hope that a dense ambient fluid may prevent the charge leakage and enable wave speed measurements to be made.

Wave speeds for Cu have been deduced from electrical measurements as described above and compared with theoretical values calculated from Equation (2). Values of liquid density, specific heat and vapor pressure were obtained from tabulated values as described in Reference 6. Owing to the scarcity of measured values of these quantities at the desired specific energies, various approximations, e.g., constancy of liquid density and specific heat, had to be made. Nevertheless, agreement between measured and calculated wave speeds for Cu³, in the temperature range from the boiling point to the critical temperature; is quite satisfactory and a considerable encouragement to further work. Accordingly, similar measurements were made on metals Al and Pb. The experimental values may be seen in Figure 3; the theoretical curve shown there comes from a thermodynamical model and assumed equation of state, see § 6.

When the tabulated data were used to calculate theoretical values⁶ for wave speeds in Pb, poor agreement with experiment was obtained and the absence of reliable high-temperature vapor pressure data for this element was thought to be responsible. Since, generally speaking, Hg is the only metal for which measurements exist of pressure, density and conductivity up to the critical temperature, there is not much hope that expected values of vaporization wave speed can be calculated for other metals with sufficient precision to provide a correct trend of the function for comparison with experimental values.

6. THERMODYNAMIC MODEL

Accordingly, we develop here a simplified fluid model to represent the transient behavior of a material heated rapidly from the solid state up through its critical temperature. Our motivation is to supply a simple yet reasonably accurate basis for describing the state and dynamical behavior of superheated liquids. In order to make any further detailed flow calculations an equation of state is needed; accordingly, the goal will be to find an approximate equation of state

which is capable of representing what is known about liquid metals and capable of filling in the large gaps where no data are available. Agreement will be sought with vaporization wave speeds, for example, even though detailed internal checks with other quantities are impossible. Our model is based on the following hypotheses: 1) the temperature rise and transitions take place under conditions of local thermodynamic equilibrium, 2) a form of van der Waals equation applies, 3) realistic specific heats can be assigned the liquid and vapor states and 4) the liquid expansion takes place along the liquidus line, $v_3(T)$ of Figure 1.

The first assumption is one mainly of simplification although a plausible argument can be given³ that vaporization from the free surface should occur nearly at equilibrium conditions.

Van der Waals equation is representative of a class of state equations which are reasonably accurate, though not precise, and yet embody the main features of most condensable gases, viz., a hard core repulsion and a weak, long-range attractive force. With the modifications to be discussed below van der Waals equation allows different and realistic specific heats to be assigned the liquid and vapor phases, a matter which improves later agreement with experiment.

Choice of the liquidus line as the thermodynamic path is somewhat arbitrary although it appears to be reasonable, as may be seen from the following argument. For most physical examples, the isotherms and adiabats in the liquid phase are very steep compared to those of either the coexistence or vapor regions, except very near the critical point. Slope magnitudes of the adiabats are proportional to sound speed squared; consequently the sound speed in the liquid is much higher than in either of the other regions. We may then argue that heating moves the thermodynamic state along the saturated liquid line. Any compressive tendency to drive the expanding system into the all-liquid state will be rapidly counteracted by liquid thermal expansion, which is dominated by the fastest speed of sound. The liquid expansion

lowers the pressure to that of the liquidus boundary where any further expansion must be accompanied, under the assumed equilibrium conditions, by partial vaporization, which is governed by the slower vaporizing wave speed. For interior parts of the system where inertial confinement prevails, premature expansion via incipient cavitation will cause local pressure rise which will force the fluid element back toward the liquidus line. This process of excursion about the liquidus continues during the electrical heating pulse until the fluid particle evaporates from the surface by expansion through the vaporization wave.

In what follows we take the thermodynamic system of interest to be a uniform, molten cylinder of metal to which heat is being added and from whose surface partial vaporization occurs. The speed of the leading edge of the vaporizing wave is assumed to proceed with the wave speed of the saturated wet vapor at absolute temperature T , as given by Equation (2) evaluated on the liquidus line.

For unit mass of fluid, pressure P and specific volume V are related by the van der Waals equation in the form

$$P_w = \hat{R}T/(V-b) - a/V^2 \quad , \quad (13)$$

where the constants a , b are given in terms of values at the critical point by

$$a = 3P_c V_c^2 \quad , \quad b = V_c/3 \quad , \quad \hat{R}T_c = (8/3) P_c V_c \quad . \quad (14)$$

Inequalities $T > 0$, $V \geq b$ are understood to hold. When $T \leq T_c$ the van der Waals equation of state describes a two-phase region where both liquid and vapor phases coexist, as in Figure 1. In the co-existence region, vapor pressure P_A is not derived directly from Equation (13) which has the form of a cubic, but rather from a generalization of the Maxwell, equal area rule which replaces the two loops by a horizontal line cutting equal areas from the loops.

G. D. Kahl¹⁰ has proven the remarkable result that the equal area condition is not necessary, but defines only one of a continuum of possible choices. For $T < T_c$ he writes

$$\int_{V_3(T)}^{V_1(T)} P_w dV = P_A(T) [V_1(T) - V_3(T)] + \phi(T) , \quad (15)$$

where

$$\phi(T) = \int_T^{T_c} [C_v(\tau, \text{liq}) - C_v(\tau, \text{vap})](1 - T/\tau) d\tau . \quad (16)$$

Specific heat at constant volume C_v is a function not only of temperature but also the state of the fluid, whether liquid or vapor. As Kahl shows, the features of equilibrium thermodynamics are preserved, the main one being the stationary property of the Gibbs function as the system passes from liquid to vapor on an isotherm. If C_v is the same for both liquid and vapor, then $\phi(T) = 0$ and Equation (15) gives the Maxwell result. If the two specific heats are not the same, then $\phi(T) \neq 0$, the areas are not equal and some further, useful flexibility is available in making a realistic choice of the two specific heat functions.

To evaluate Equation (2) for the vaporization sound speed on the liquidus line, P_A and $V_3 = 1/\rho_3$ can be found numerically from Equations (15) and (16). The specific heat for the coexistence state, C_{vA} , must also be found formally and then numerically. To do this one finds the internal energy E_A and differentiates, using $C_{vA} = (\partial E_A / \partial T)_v$. E_A may be determined from the general relation

$$(\partial E / \partial V)_T = T(\partial P / \partial T)_V - P \quad , \quad (17)$$

and noting from Equation (15) that $M(T) = T(\partial P_A / \partial T)_V - P_A$ is independent of V . Direct integration of Equation (17) gives

$$E_A = E_w + M(T)[V - V_3(T)] \quad , \quad (18)$$

where $E_W = E_W(V_3, T)$ is the internal energy on the liquidus given by the van der Waals function. One finds

$$C_{VA} = (\partial E_W / \partial T)_V + (dM/dT)(V - V_3) - M (dV_3 / dT) , \quad (19)$$

and

$$(\partial E_W / \partial T)_V = (\partial E_W / \partial V_3)_T (dV_3 / dT) + (\partial E_W / \partial T)_V ; \quad (20)$$

finally, on the saturated liquid line

$$C_{VA} = [(\partial E_W / \partial V_3)_T - M] (dV_3 / dT) + (\partial E_W / \partial T)_V . \quad (21)$$

The last term is $C_V(T, liq)$ and may be taken from experiment or represented approximately in some chosen functional form. Van der Waals equation gives no further information. Putting P_W in Equation (17) gives $\partial E_W / \partial V_3 = a/V_3^2$. With these results, Equations (15), (16), (21) and van der Waals equation, the vaporization wave speed can be numerically evaluated on $V_3(T)$. In the liquid the more general definition of Equation (1) must be used.

While the equation of state is expressed in terms of absolute temperature, the independent variable one obtains more easily from experiment is the added specific heat content Δq . One can make the connection between q and T by integrating $dq = dE + pdV$ along $V_3(T)$ from the melting temperature T_M to T using computed values of $E_W(V_3, T)$ and $P_A(T)$. For any $T \leq T_c$ a correspondence is thus given between $\Delta q(T)$ and T . One then writes $q(T) = q(T_M) + \Delta q(T)$ where $q(T_M) = q_M$ is the heat content of the liquid at melt, assumed known from other sources. Clearly the scaled variable $\bar{q} = q / \hat{R}T_c$ depends upon the specific heats of the liquid and vapor phases through Equations (15) and (16), as well as on $q_M / \hat{R}T_c$. This latter quantity has a value near 0.60 for a number of metals. Both scaled wave speed $\bar{c} = C_W / (\hat{R}T_c)^{\frac{1}{2}}$ and scaled heat content are functionals of the specific heats for liquid and vapor. When one can approximate both of the specific heat functions by constants, the parametric dependence of the wave speed curve on the choices of specific heats can readily be shown as in Reference 9.

7. COMPARISON OF THE THERMODYNAMIC MODEL WITH EXPERIMENT

Wave speed data for six metals, Au, Ag, Cu, Al, Pb, Hg, are displayed in Figure 3. While a somewhat similar plot appears in Reference 9 where cross-hatched areas are used to represent the more abundant data, here the individual data points are included for a range of variables which includes most of the two-phase field. Dimensionless wave speeds \bar{c} are plotted against dimensionless specific heat content \bar{q} . Because measured, thermal expansion data for liquid metals are lacking, no correction could be made for the effects expansion prior to the passage of the vaporization wave. Likewise, no measured values of critical point data are available for any metal except Hg so the best recent estimates were used.^{11,12,13} The scaling constants are summarized in Table I.

Table I. Scaling Constants

<u>Metal</u>	<u>T_m</u> °K	<u>T_c</u> °K	<u>$\hat{R}T_c$</u> kJ/gm	<u>$(\hat{R}T_c)^{\frac{1}{2}}$</u> m/sec
Al	933	8650	2.67	1633
Cu	1356	8500	1.09	1043
Ag	123 ⁴	7460	0.575	758
Au	1336	9500	0.401	630
Hg	23 ⁴	1733	0.0718	268
Pb	601	5400	0.217	465

The theoretical curve is computed from a modified van der Waals model, in dimensionless form, with critical compressibility 3/8, and with $C_v(\text{liq}) = (5/2)\hat{R}$ and $C_v(\text{vap}) = (3/2)\hat{R}$. This choice of specific heats, made possible by relinquishing Maxwell's equal area rule, is a better approximation to the known specific heat data than

assumption of identical specific heats for liquid and vapor. In its scaled form \bar{c} is then a function of dimensionless variables only.

The scale of reduced specific heat content, \bar{q} , for the theoretical curve is that computed from the van der Waals function, with an added 0.1 unit to adjust the \bar{q}_M value so that it represents, reasonably well, the corresponding values for the six metals which cluster fairly closely to the nominal, empirical value of 0.60

As may be seen in Figure 3 the data and the theoretical curve agree quite well on the point of inception of vaporization wave speed, and on the early rise of the curve. The data points for the noble metals fall below the theoretical curve and go out beyond the critical point limit toward what appears to be a horizontal asymptote. Handbook wave speeds for Cu³ actually agree better with the plotted data than does the van der Waals curve. Some recent unpublished data on Cu taken in our laboratory, reduced by a finer-grained method of reduction, adhere more closely to the van der Waals curve up to an ordinate of 0.15 before bending away. If the correction for thermal expansion could be applied, the wave speed values would be increased by at least 20 - 70% depending on \bar{q} , the larger increases applying near critical. Such a correction would somewhat improve the agreement for Ag, Cu, Au and Al; but would move Pb and Hg points further away from the theoretical curve.

Some especial problems were encountered with the Hg wires which had to be frozen in an acetone dry-ice mixture, kept in a cold box and transferred rapidly to the test cell for explosion. Refinements in this process might result in better reproducibility of the mercury data.

8. DEVIATIONS FROM THE MODEL

If we confine our attention to phenomena below critical, two deviations from the assumed model appear to be of primary importance.

The theoretical wave speed applies to the head of an expansion wave traveling into the molten fluid. Of necessity the front across which the conductivity drops to zero must come somewhere in the region of reduced density behind the head of the wave. It may occur across a narrow segment of the expansion fan and thus be representable by a sharp front possibly resembling a "conductivity shock wave," but its speed of propagation will be less than that of the sound wave which first travels into the interior. Because we know little about the change of conductivity in the expansion wave we have no way of estimating the decrement in wave speeds to be expected. The noble metals and Al fall below the theoretical curve in the expected way but Pb and Hg do not.

The x-ray pictures of Fansler and Shear¹⁴ demonstrate that for wires 2 - 5 times larger and for somewhat slower rates of energy addition the expanding cylinder of molten fluid is not uniform but displays the transverse variations in density called striations. How these striations are related to the expansion wave is not known at present although some speculative hypotheses can be advanced. Their presence in these cases appears to rule out the hypothesis that the vaporization wave always proceeds uniformly through a cylinder of uniform density.

The effect of unvaporized portions of the wire remaining in striations appears to move all data points toward higher values of q by variable amounts. There is presently no method of estimating this effect. Experiments now underway are directed toward determining the relationship between number of striations and rate of energy addition during vaporization wave passage. The present x-ray techniques are unable to resolve any striations in the smaller wires

and faster explosions typical of much of the data plotted in Figure 3; however, their presence in the larger, slower cases is a cautionary warning that density variations somehow play an important part in the heating and expansion of superheated metals.

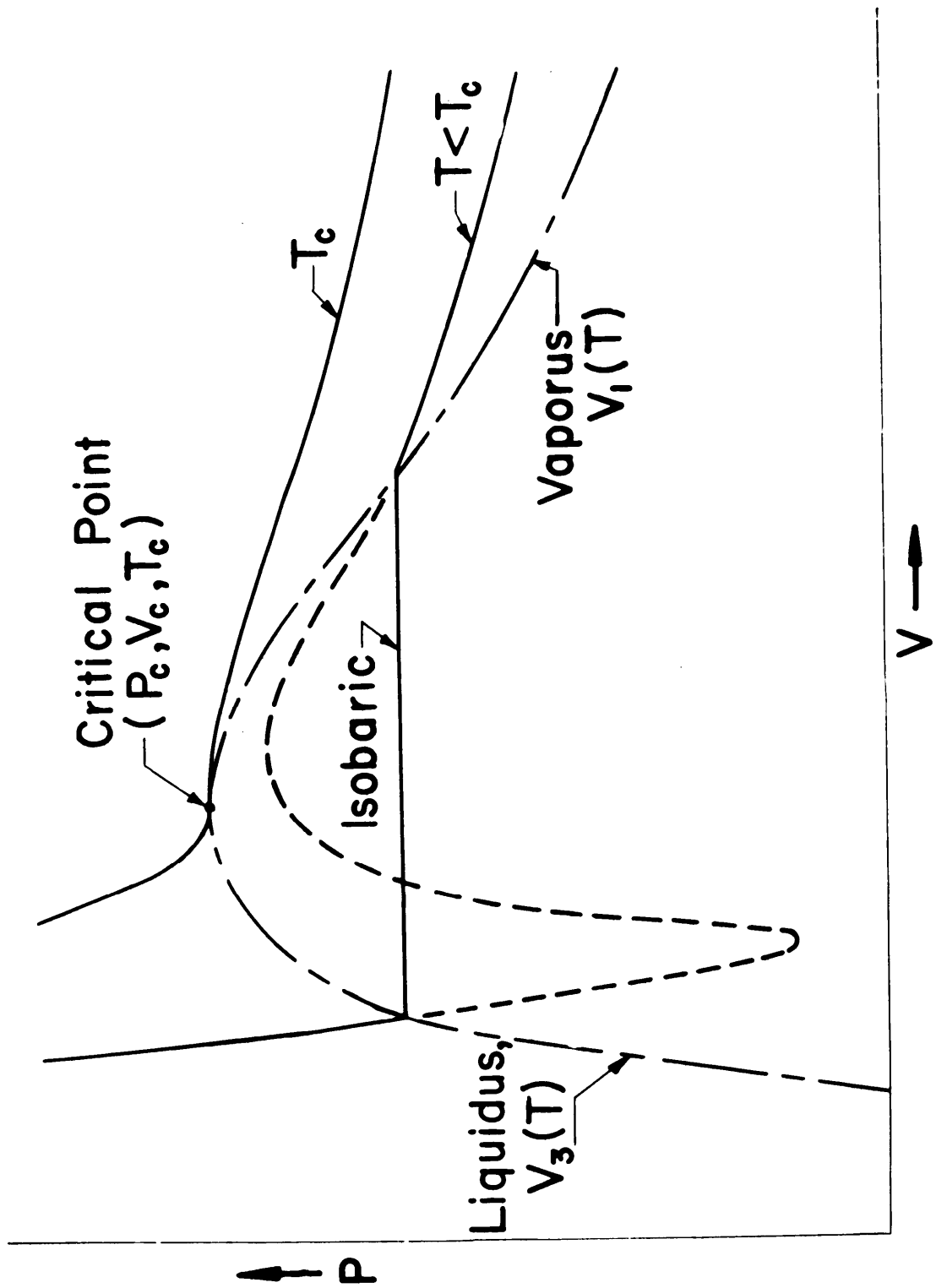


Figure 1. Sketch of two-phase region and isotherms.
 P - pressure, V - specific volume.

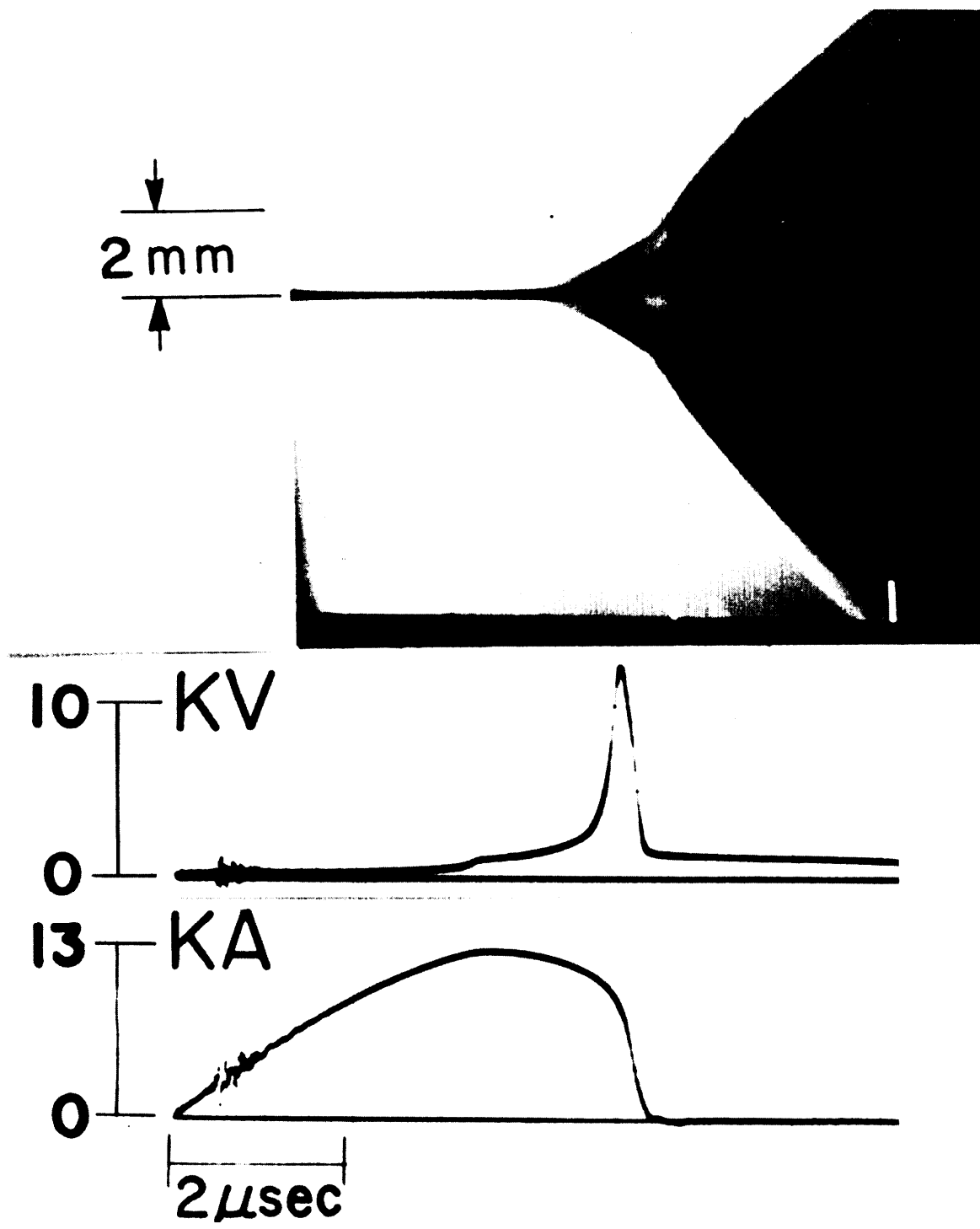


Figure 2. Streak photograph of expanding copper wire correlated in time with current and voltage.
 $d = .0254 \text{ cm}$, $V_0 = 3 \text{ kV}$, $C = 32 \mu\text{F}$.

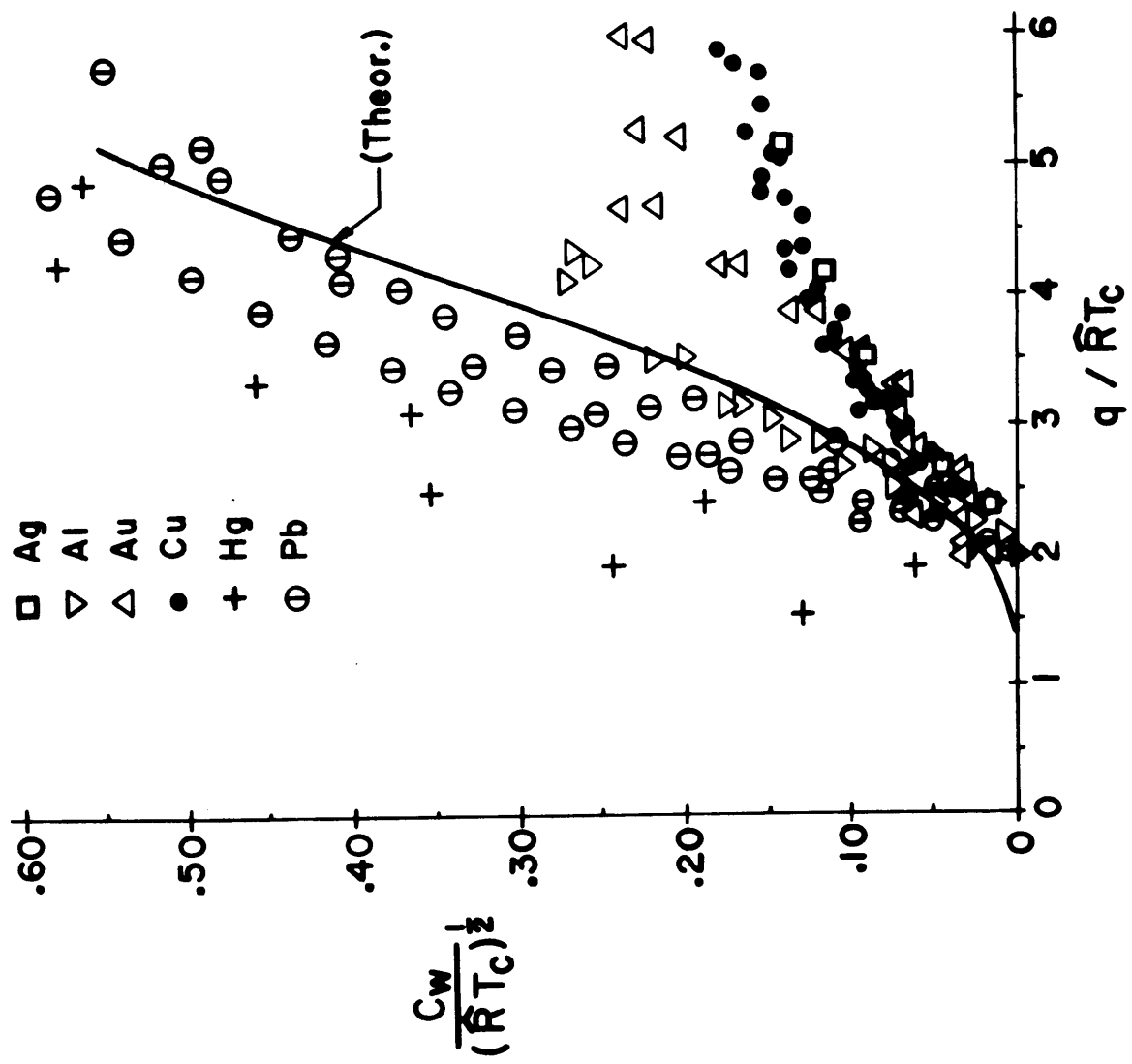


Figure 3. Wave speeds for several metals.

REFERENCES

1. R. Courant and K. O. Friedrichs, Supersonic Flow and Shock Waves, Interscience Publishers, Inc., New York (1948), pp. 92-105.
2. C. F. Curtiss, C. A. Boyd and H. B. Palmer, J. Chem. Phys. 19, 801 (1951).
3. F. D. Bennett, G. D. Kahl and E. H. Wedemeyer in Exploding Wires, Vol. 3, edited by W. G. Chace and H. K. Moore, Plenum Press, New York (1964), pp. 80-82.
4. E. A. Brown, Jr., Explosive Decompression of Water, PhD Thesis, Northwestern University, Evanston, Illinois (1959).
5. T. E. Terner, Ind. Eng. Chem., Process Design Dev. 1, 84 (1962).
6. F. D. Bennett, Phys. Fluids 8, 1425 (1965).
7. F. D. Bennett, "High Temperature Exploding Wires" in Progress in High Temperature Physics and Chemistry, Vol. 2, edited by C. A. Rouse, Pergamon Press, London (1968), pp. 1-63.
8. ibid. p. 29.
9. F. D. Bennett and G. D. Kahl in Exploding Wires, Vol. 4, edited by W. G. Chace and H. K. Moore, Plenum Press, New York (1968).
10. G. D. Kahl, Phys. Rev. 155, 78 (1967).
11. A. v. Grosse, J. Inorg. Nucl. Chem. 22, 23 (1961).
12. J. A. Cahill and A. D. Kirshenbaum, J. Phys. Chem. 66, 1050 (1962).
13. A. v. Grosse, Rev. Hautes Temp. et. Refract. 3(2), 115 (1966).
14. K. S. Fansler and D. D. Shear, Exploding Wires, Vol. 4 edited by W. G. Chace and H. K. Moore, Plenum Press, New York (1968), p. 185.

DISTRIBUTION LIST

<u>No. of Copies</u>	<u>Organization</u>	<u>No. of Copies</u>	<u>Organization</u>
20	Commander Defense Documentation Center ATTN: TIPCR Cameron Station Alexandria, Virginia 22314	1	Commanding Officer U.S. Army Picatinny Arsenal ATTN: SMUPA-V, Mr. E. Walbrecht Dover, New Jersey 07801
1	Commanding General U.S. Army Materiel Command ATTN: AMCRD-TE Washington, D.C. 20315	1	Commanding Officer U.S. Army Harry Diamond Laboratories Washington, D.C. 20438
1	Commanding General U.S. Army Materiel Command ATTN: AMCRD-TP Washington, D.C. 20315	1	Commandant U.S. Army Logistics Management Center Fort Lee, Virginia 23801
1	Commanding General U.S. Army Materiel Command ATTN: AMCRD-BN Washington, D.C. 20315	1	Commanding Officer U.S. Army Materials and Mechanics Research Center Watertown, Massachusetts 02712
2	Commanding General U.S. Army Missile Command ATTN: AMSMI-RBL Redstone Arsenal, Alabama 35809	1	Commanding General U.S. Army Natick Laboratories Natick, Massachusetts 01762
1	Commanding Officer U.S. Army Mobility Equipment Research and Development Center ATTN: Tech Docu Cen, Bldg 315 Fort Belvoir, Virginia 22060	1	Commanding Officer U.S. Army Foreign Science and Technology Center Munitions Building Washington, D.C. 20315
2	Commanding Officer U.S. Army Frankford Arsenal ATTN: SMUFA-N1000, Mr. Lukens SMUFA-C2500 Philadelphia, Pennsylvania 19137	1	Commanding Officer U.S. Army Cold Regions Research and Engineering Laboratories Hanover, New Hampshire 03755
		1	Commanding Officer U.S. Army Satellite Communications Agency Fort Monmouth, New Jersey 07703
		1	Commanding Officer U.S. Army Maintenance Board Fort Knox, Kentucky 40121

DISTRIBUTION LIST

<u>No. of Copies</u>	<u>Organization</u>	<u>No. of Copies</u>	<u>Organization</u>
1	Commanding General U.S. Army Combat Developments Command ATTN: CDCMR-W Fort Belvoir, Virginia 22060	1	Superintendent U.S. Naval Postgraduate School ATTN: Tech Rept Sec Monterey, California 93940
1	Office of Vice Chief of Staff ATTN: CSAVCS-W-TIS Department of the Army Washington, D.C. 20310	3	Director U.S. Naval Research Laboratory ATTN: Code 7700, Dr. A. Kolb Code 7720, Dr. E. McLean; Mr. I. Vitkovitsky Washington, D.C. 20390
1	Director U.S. Army Research Office 3045 Columbia Pike Arlington, Virginia 22204	1	Commander U.S. Naval Weapons Laboratory Dahlgren, Virginia 22448
1	Commanding Officer U.S. Army Research Office - Durham Box CM, Duke Station Durham, N. C. 27706	1	ADTC (ADBPS-12) Eglin AFB Florida 32542
3	Commander U.S. Naval Air Systems Command ATTN: AIR-604 Washington, D.C. 20360	1	ADTC (PGOW) Eglin AFB Florida 32542
3	Commander U.S. Naval Ordnance Systems Command ATTN: ORD-9132 Washington, D.C. 20360	1	AFATL (ATW) Eglin AFB Florida 32542
1	Commander U.S. Naval Weapons Center ATTN: Code 753 China Lake, Calif. 93555	1	AFWL (WLRE, Dr. Guenther) Kirtland AFB New Mexico 87117
2	Commander U.S. Naval Ordnance Laboratory ATTN: Code 730, Lib Code 242, Mr. H. Leopold Silver Spring, Md. 20910	1	AUL (3T-AUL-60-118) Maxwell AFB Alabama 36112
		1	AFAL (AVW) Wright-Patterson AFB Ohio 45433

DISTRIBUTION LIST

<u>No. of Copies</u>	<u>Organization</u>	<u>No. of Copies</u>	<u>Organization</u>
3	Director National Bureau of Standards ATTN: Dr. D. Tsai Mr. P. Krupenie Mr. J. Park U.S. Department of Commerce Washington, D.C. 20235	1	Director National Aeronautics and Space Administration Electronics Research Center ATTN: Dr. V. Scherrer 575 Technology Square Cambridge, Mass. 02139
1	Headquarters U.S. Atomic Energy Commission ATTN: Lib Br Washington, D.C. 20545	1	Director National Aeronautics and Space Administration Langley Research Center ATTN: Code 04.000 Langley Station Hampton, Virginia 23365
3	Director U.S. Atomic Energy Commission ATTN: Tech Info Div P.O. Box 62 Oak Ridge, Tennessee 37831	1	Director National Aeronautics and Space Administration Lewis Research Center 21000 Brookpark Road Cleveland, Ohio 44135
1	Director Lawrence Radiation Laboratory ATTN: Dr. C. Olsen P.O. Box 808 Livermore, California 94550	1	Director Jet Propulsion Laboratory ATTN: Mr. I. Newlan 4800 Oak Grove Drive Pasadena, California 91103
2	Director Los Alamos Scientific Laboratory ATTN: Dr. R. Reithel Dr. J. L. Tuck P.O. Box 1663 Los Alamos, New Mexico 87544	1	Director Smithsonian Astrophysical Observatory 60 Garden Street Cambridge, Mass. 01238
1	Director NASA Scientific and Technical Information Facility ATTN: SAK/DL P.O. Box 33 College Park, Maryland 20740	1	Aerojet-General Corporation ATTN: Dr. G. Woffinden 11711 South Woodruff Avenue Downey, California 90241

DISTRIBUTION LIST

<u>No. of Copies</u>	<u>Organization</u>	<u>No. of Copies</u>	<u>Organization</u>
1	Atlantic Research Corporation ATTN: Mr. A. Macek Shirley Highway at Edsall Rd Alexandria, Virginia 22314	1	General Precision, Inc. General Precision Laboratory Division 63 Bedford Road Pleasantville, New York 10570
2	AVCO-Everett Research Laboratory ATTN: Tech Lib Dr. G. Sargent James 2385 Revere Beach Parkway Everett, Massachusetts 02149	1	Hughes Aircraft Company Systems Development Laboratory ATTN: Dr. A. Puckett Florence and Teale Streets Culver City, California 90230
1	E.I. duPont de Nemours and Company Eastern Laboratory Library ATTN: Miss M. Imbrie Gibbstown, New Jersey 08027	1	Lockheed Missile and Space Company 3251 Hanover Street Palo Alto, California 94304
1	Fairchild Hiller Republic Aviation Division ATTN: Engr Lib Farmingdale, New York 11735	1	North American Rockwell Corporation Space Division ATTN: Dr. J. O'Keefe 1221 ⁴ Lakewood Boulevard Downey, California 90241
2	Field Emission Corporation ATTN: Mr. F. Collins Dr. J. Trolan McMinnville, Oregon 97128	1	Radio Corporation of America RCA Laboratories Division ATTN: Dr. H. Hendel Princeton, New Jersey 08540
1	General Electric Research Laboratory ATTN: Dr. R. Alpher P.O. Box 1088 Schenectady, New York 12305	2	Sandia Corporation ATTN: Mr. J. R. Hearst Building T105 Dr. G. Anderson P.O. Box 969 Livermore, California 94551
1	General Electric Company General Engineering Laboratory P.O. Box 11 Schenectady, New York 12305	3	Sandia Corporation ATTN: Dr. E. Cnare Dr. F. Neilson Dr. T. Tucker P.O. Box 5800 Albuquerque, New Mexico 87115
1	General Electric Company Space Sciences Laboratory ATTN: Dr. R. Good, Jr. P.O. Box 8555 Philadelphia, Pa. 19101		

DISTRIBUTION LIST

<u>No. of Copies</u>	<u>Organization</u>	<u>No. of Copies</u>	<u>Organization</u>
1	Shock Hydrodynamics, Inc. ATTN: Dr. L. Zernow 15010 Ventura Boulevard Sherman Oaks, California 91403	1	University of California Department of Chemistry ATTN: Dr. G. Nash Davis, California 95616
1	Arizona State University ATTN: Professor R. Stoner Tempe, Arizona 85281	1	University of California Department of Mechanical Engineering ATTN: Professor S. Schaaf Berkeley, California 94704
1	University of Arkansas Department of Physics ATTN: Professor O. Zinke Fayetteville, Arkansas 72701	1	Columbia University ATTN: Professor R. Gross 236 Seeley W. Mudd Building New York, New York 10027
1	California Institute of Technology Guggenheim Aeronautical Laboratory ATTN: Professor L. Lees Pasadena, California 91104	1	University of Colorado Joint Institute for Laboratory Astrophysics ATTN: Professor R. Thomas 1511 University Avenue Boulder, Colorado 80304
1	California Institute of Technology Aeronautics Department ATTN: Professor H. Liepmann 1201 East California Blvd. Pasadena, California 91102	1	Cornell University Graduate School of Aeronautical Engineering ATTN: Professor E. Resler Ithaca, New York 14850
1	California Institute of Technology Firestone Flight Sciences Laboratory ATTN: Professor G. Whitham Pasadena, California 91104	1	Cornell Aeronautical Laboratory, Inc. ATTN: Lib P.O. Box 235 Buffalo, New York 14221
1	Case Institute of Technology Department of Mechanical Engineering ATTN: Professor G. Kuerti 10900 Euclid Avenue Cleveland, Ohio 44106	1	Cornell Aeronautical Laboratory, Inc. ATTN: Dr. G. Skinner P.O. Box 235 Buffalo, New York 14221

DISTRIBUTION LIST

<u>No. of Copies</u>	<u>Organization</u>	<u>No. of Copies</u>	<u>Organization</u>
1	Hartford Graduate Center R.P.I. ATTN: Professor R. Campbell East Windsor Hill, Conn. 06028	2	University of Maryland Institute of Fluid Dynamics and Applied Mathematics ATTN: Professor J. Burgers Professor S. Pai College Park, Maryland 20740
1	Harvard University ATTN: Professor H. Emmons Cambridge, Mass. 02138	1	Massachusetts Institute of Technology Aerophysics Laboratory Cambridge, Mass. 02139
1	University of Houston Department of Physics ATTN: Dr. D. Ross Cullen Boulevard Houston, Texas 77004	1	Willow Run Laboratories ATTN: Tech Docu Svcs P.O. Box 2008 Ann Arbor, Michigan 48104
1	IIT Research Institute ATTN: Dr. Robert Dennen 10 West 35th Street Chicago, Illinois 60616	1	University of Michigan Department of Physics ATTN: Professor O. Laporte Ann Arbor, Michigan 48104
1	University of Illinois Department of Aeronautical Engineering ATTN: Professor R. Strehlow Urbana, Illinois 61803	2	University of Michigan Gas Dynamics Laboratories ATTN: Mr. E. Oktay Professor P. Sherman North Campus, Building 422 Ann Arbor, Michigan 48105
1	Director Applied Physics Laboratory The Johns Hopkins University 8621 Georgia Avenue Silver Spring, Maryland 20910	1	University of Michigan Department of Aeronautical and Astronautical Engineering ATTN: Professor M. Sichel Ann Arbor, Michigan 48104
1	The Johns Hopkins University Department of Mechanics ATTN: Professor L. Kovasznay 34th and Charles Street Baltimore, Maryland 21218	1	North Carolina State University at Raleigh ATTN: Dr. Tien S. Chang 325 Riddick Laboratories Raleigh, North Carolina 27607
1	Lehigh University Department of Physics ATTN: Professor R. Emrich Bethlehem, Pa. 18015		

DISTRIBUTION LIST

<u>No. of Copies</u>	<u>Organization</u>	<u>No. of Copies</u>	<u>Organization</u>
1	Northern Illinois University ATTN: Professor M. Joncich DeKalb, Illinois 60115	1	University of Southern California Engineering Center ATTN: Professor R. Binder Los Angeles, Calif. 90007
1	Oklahoma City University Department of Physics ATTN: Professor M. Coffman Oklahoma City, Oklahoma 73100	1	Stanford University Department of Mechanical Engineering ATTN: Professor D. Bershadier Stanford, California 94305
1	University of Oklahoma Department of Physics ATTN: Professor R. Fowler Norman, Oklahoma 73069	1	Stevens Institute of Technology Department of Electrical Engineering ATTN: Professor R. Geldmacher Castle Point Station Hoboken, New Jersey 07030
1	University of Pennsylvania The Towne School of Civil and Mechanical Engineering ATTN: Professor Ira M. Cohen Philadelphia, Pa. 19104	1	Syracuse University Department of Physics ATTN: Professor C. Bachman Syracuse, New York 13201
1	University of Pennsylvania Moore School of Electrical Engineering ATTN: Professor S. Gorn Philadelphia, Pa. 19104	1	Syracuse University Mechanical Engineering Dept ATTN: Professor D. Dosanjh Syracuse, New York 13201
1	Princeton University Palmer Physical Laboratory ATTN: Professor W. Bleakney Princeton, New Jersey 08540	1	Temple University Department of Physics ATTN: Professor T. Korneff Philadelphia, Pa. 19122
1	Princeton University Department of Aerospace and Mechanical Sciences ATTN: Professor W. D. Hayes Princeton, New Jersey 08540	1	Yeshiva University Graduate School of Mathematical Sciences ATTN: Mr. Z. Rieder Amsterdam Avenue and 186th Street New York, New York 10033
1	Princeton University Forrestal Research Center ATTN: Professor S. Bogdonoff Princeton, New Jersey 08540		

DISTRIBUTION LIST

<u>No. of</u>	<u>Copies</u>	<u>Organization</u>
---------------	---------------	---------------------

Aberdeen Proving Ground

Chief, Tech Lib
Marine Corps Ln Off
CDC Ln Off

UNCLASSIFIED

Security Classification

DOCUMENT CONTROL DATA - R & D

(Security classification of title, body of abstract and indexing annotation must be entered when the overall report is classified)

1. ORIGINATING ACTIVITY (Corporate author) U. S. Army Aberdeen Research and Development Center Ballistic Research Laboratories Aberdeen Proving Ground, Maryland		2a. REPORT SECURITY CLASSIFICATION UNCLASSIFIED
		2b. GROUP
3. REPORT TITLE VAPORIZATION WAVE TRANSITIONS		
4. DESCRIPTIVE NOTES (Type of report and inclusive dates)		
5. AUTHOR(S) (First name, middle initial, last name) F. D. Bennett		
6. REPORT DATE November 1969	7a. TOTAL NO. OF PAGES 38	7b. NO. OF REFS 14
8a. CONTRACT OR GRANT NO.	9a. ORIGINATOR'S REPORT NUMBER(S) Report No. 1456	
b. PROJECT NO. RDT&E Project No. 1T061102A33D	9b. OTHER REPORT NO(S) (Any other numbers that may be assigned this report)	
c.		
d.		
10. DISTRIBUTION STATEMENT This document has been approved for public release and sale; its distribution is unlimited.		
11. SUPPLEMENTARY NOTES	12. SPONSORING MILITARY ACTIVITY U. S. Army Materiel Command Washington, D. C.	
13. ABSTRACT A vaporization wave analogous to the unsteady simple wave in an expanding gas is proposed to account for phenomena observed in the evaporation of superheated metals. The vaporizing model is visualized on thermodynamic grounds as carrying the liquid metal through a continuous succession of states either on or near the liquidus line in the two-phase region. On this line, the adiabatic sound speed for wet vapor will limit the rate of propagation of the vaporization front into the liquid. Experimental data for wire explosions of Al, Ag, Cu, Au, Pb, and Hg (frozen) are analyzed for wave speeds. While the influence of thermal expansion of the liquid can be accounted for theoretically, insufficient thermal data are available for the metals to permit correction of the wave speeds for this effect. The experimentally derived wave speeds are compared with theoretical values of the adiabatic sound speed in the wet vapor obtained from a modified van der Waals equation of state. At low velocities, the agreement is satisfactory but higher values deviate considerably from theory. Possible causes of the deviations include the crudity of the fluid dynamic model, neglect of thermal expansion, lack of information about the relationship between density and electrical conductivity and the approximation imposed by the van der Waals equation.		

UNCLASSIFIED

Security Classification

14. KEY WORDS	LINK A		LINK B		LINK C	
	ROLE	WT	ROLE	WT	ROLE	WT
Vaporization Waves Fluid Dynamics High Temperature Metals Unsteady Flows Simple Waves Critical Phenomena						

UNCLASSIFIED

Security Classification